frontiers | Frontiers in Energy Research

TYPE Original Research
PUBLISHED 08 January 2024
DOI 10.3389/fenrg.2023.1348557

OPEN ACCESS

EDITED BY
Meng Jia,
Shandong University of Science and Technology, China

REVIEWED BY
Ziming Liu,
Tongji University, China
Jiaming Wu,
University of Jinan, China

*CORRESPONDENCE
Chuanhai Li,
15665716260@163.com

RECEIVED 03 December 2023
ACCEPTED 18 December 2023
PUBLISHED 08 January 2024

CITATION
Chu F, Li C, Wu C and Wang Y (2024), Research on the hydration process of solid waste–based cementitious materials and application in roadbase.
Front. Energy Res. 11:1348557.
doi: 10.3389/fenrg.2023.1348557

Research on the hydration process of solid waste–based cementitious materials and application in roadbase

Feng Chu[1], Chuanhai Li[2]*, Chuanshan Wu[1] and Yansheng Wang[3]

[1]Shandong Hi-speed Construction Management Group Co., Ltd., Jinan, China, [2]Shandong Hi-Speed Engineering Testing Co., Ltd., Jinan, China, [3]Geotechnical and Structural Engineering Research Center, Shandong University, Jinan, China

In order to improve the high-value utilization of industrial solid waste materials, this study prepared a solid waste–based cementitious material (SWCM) using slag, fly ash, desulfurization gypsum, and gangue. The mechanical strength and hydration process of the SWCM and an ordinary Portland cement (OPC) were studied. The results showed that the compressive strength of the SWCM was lower than that of OPC at 3 d, but the compressive strength exceeded that of OPC after 7 d. The isothermal calorimetry results showed that the induction period of the SWCM was five times that of OPC, and the total 4 d exothermic amount of OPC was 1.7 times that of the SWCM. XRD and SEM showed that the hydration products of the SWCM were mainly ettringite (AFt) and hydrated calcium silicate gel (C-S-H). The unconfined compressive strength and dry shrinkage of stabilized macadam were also studied by using the SWCM to replace OPC. The results indicated that the unconfined compressive strength of the SWCM-stabilized macadam is comparable to that of the OPC-stabilized macadam. The dry shrinkage strain was only 79.7% of the OPC-stabilized macadam.

KEYWORDS

SWCM, strength, microscopic characteristics, SWCM-stabilized macadam, unconfined compressive strength, flexural strength, dry shrinkage

1 Introduction

Portland cement is widely used in infrastructure construction due to abundance of its raw materials and low price, especially in the semi-rigid base layer of pavements (Dobiszewska et al., 2023; Griffiths et al., 2023; Guo et al., 2023). It has been estimated that more than 4,000 tons of cement is used for each kilometer of high-grade asphalt pavement base (Wiranata et al., 2022). The production of large quantities of Portland cement brings economic benefits while posing serious challenges to natural resources and the environment. Over the past few years, a great deal of attention has been given to the development of specialty cementitious materials that can reduce CO_2 emissions and lower energy and limestone consumption (Mo et al., 2017; Zhang et al., 2021; Sun et al., 2022a). At the same time, with the accelerating process of modernization, the emission of granulated blast furnace slag, desulfurization gypsum, fly ash, and other industrial solid wastes continues to increase (Zhao et al., 2016; Zhao et al., 2022; Xu et al., 2023). It is imperative to carry out the utilization of industrial solid waste to prepare environmentally friendly cementitious materials.

TABLE 1 Chemical content of raw materials (w/%).

	CaO	SiO_2	Al_2O_3	MgO	Fe_2O_3	SO_3	Loss
S95 Slag	44.71	29.29	14.85	7.33	0.39	1.28	2.15
Gangue	3.44	49.93	36.17	0.80	5.79	1.12	2.75
Desulfurization gypsum	35.35	1.56	0.80	0.35	0.12	44.74	17.08
Cement clinker	63.21	21.06	6.74	3.24	3.45	0.58	1.72

Granulated blast furnace slag is an industrial by-product obtained by quenching and cooling the molten residue of combustion in the ironmaking process, which has been widely used because of its high pozzolanic activity and latent hydraulicity (Matthes et al., 2018). As a typical aluminum silicate mineral, the main composition of slag is similar to that of Portland cement clinker, which is mainly a compound of CaO-Al_2O_3-SiO_2-MgO. With the increase in CaO and Al_2O_3, the contents of SiO_2 and TiO_2 decrease in slag, and the hydration process is gradually enhanced (Wang et al., 2022). Desulfurization gypsum is a by-product of flue gas desulfurization in power plants; the main component is $CaSO_4{\cdot}2H_2O$ (Koralegedara et al., 2019). Fly ash is the main solid waste from coal-fired power plants. Fly ash, as an additive to concrete, improves the plasticity and fluidity of concrete and increases its strength and durability (Grabias-Blicharz and Franus, 2023). In recent years, some studies have been conducted on the mechanism of shrinkage and enhancement behavior of desulfurization gypsum–slag–cement cementitious material for stabilized macadam (Li et al., 2017; Ju et al., 2019; Ou-Ming et al., 2019; Deng et al., 2020; Qing-qing, 2021; Qian et al., 2022). The results show that gypsum can promote the hydration reaction of slag. Besides, gypsum can promote the generation of ettringite (AFt) to achieve the micro-expansion of the volume to reduce shrinkage and deformation. Qing-qing (2021) found that compounding of fly ash and slag improved the mechanical properties and shrinkage characteristics of cement-stabilized macadam significantly. Ou-Ming et al. (2019) found that early strength and dry shrinkage could be improved by adding slag and gypsum to cement–lime–fly ash-stabilized macadam. The results show that the pozzolanic reaction is between slag and lime, and the dihydrate gypsum leads to the formation of a large number of AFt. At present, the technology of preparing solid waste–based cementitious materials (SWCMs) based on multi-source solid waste is becoming increasingly widespread, and the application of solid waste–based cementitious materials in road engineering is becoming more and more extensive.

In this study, S95 slag, desulfurization gypsum, and gangue were first used as the main components to prepare solid waste–based cementitious materials (SWCMs), and mechanical strength, hydration process, and hydration products were investigated. Then, the SWCM was used to prepare stabilized macadam materials, and the unconfined compressive strength, flexural strength, and dry shrinkage were studied. The research results provide a basis for the high-value utilization of solid waste materials. The use of SWCM has excellent mechanical strength and smaller dry shrinkage strain, providing reference for the design and performance evaluation of stabilized macadam.

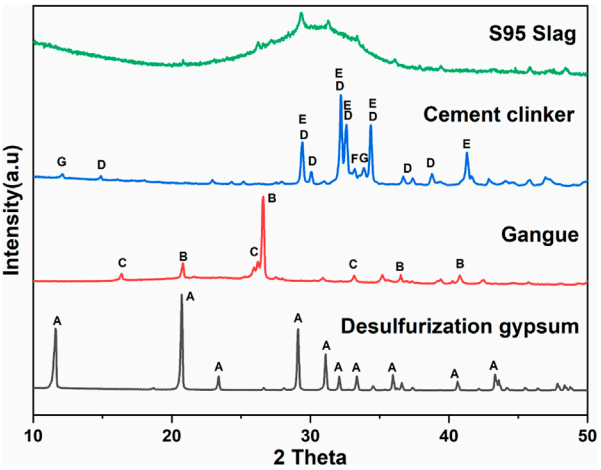

FIGURE 1
The XRD pattern of raw materials (A: $CaSO_4{\cdot}2H_2O$, B: SiO_2, C: Mullite, D: Alite, E: Belite, F: C_3A, and G: C_4AF).

2 Experimental program

2.1 Raw materials

S95 slag, desulfurization gypsum, gangue, and cement clinker were adopted in the experiment. The chemical compositions and mineral components are shown in Table 1 and Figure 1, respectively.

2.2 SWCM preparation and test procedure

2.2.1 Physical properties

According to the composition of the SWCM given in Table 2, the various types of raw materials in accordance with the proportion of mixing were ground in the ball mill for 1 h to obtain SWCM. The specimens were prepared in the size of 40 mm × 40 mm × 160 mm for mechanical properties according to the Chinese standard GB/T17671-1999 "Method of testing cements–Determination of strength". The samples were demolded after 48 h, and then maintained in water at 20°C ± 1°C. The compressive strength and flexural strengths were tested at 3 d, 7 d, and 28 d.

2.2.2 Calorimetry

The hydration heat evolution rate and total hydration heat emission of cementitious materials were measured by using an isothermal calorimeter (TAM Air) at 25 C within 100 h. All the experiments were performed at a W/C = 0.5 by mass. Furthermore,

TABLE 2 Composition of SWCM.

	Cement clinker	S95 slag	Gangue	Desulfurization gypsum
Proportion (%)	5	63	20	12

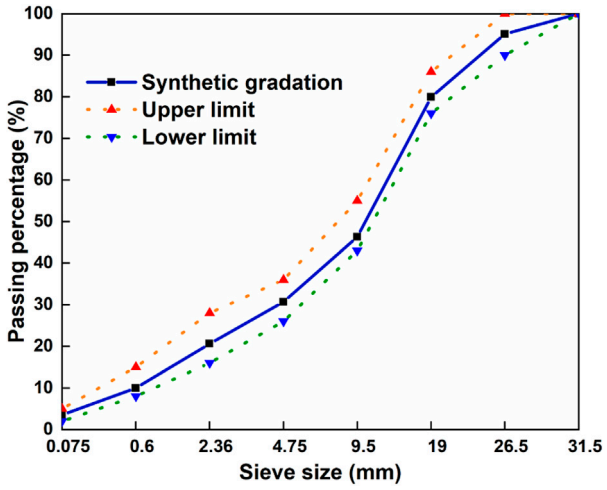

FIGURE 2
Gradation of mixtures.

2 g cement and 1 g water were placed into standard glass bottles and then put in the device. Then, the mixture was stirred quickly and put into the chamber to measure hydration heat.

2.2.3 Microstructure analysis

Sand-free hardened paste samples at 7 d and 28 d were taken for testing. The samples were immersed in anhydrous ethanol for 48 h to terminate the hydration reaction and then dried at 40°C for 48 h. XRD data were collected by using the Bruker AXS D8 Advance diffractometer device and collected in 2θ from 10° to 60°. SEM images were investigated using a Zeiss field emission scanning electron microscope.

2.3 Mixture preparation and experimental program

2.3.1 Mixture and sample preparation

Skeleton-dense gradation was used for preparing cement-stabilized macadam, and the gradation curve is shown in Figure 2. The cementitious materials were selected as 3%, 4%, 5%, and 6% by weight of the total aggregates. The mixed samples were compacted at different water content by using compaction methods in the Chinese standard JTG E51-2009. The optimum water content was determined on the basis of the curve of water content *versus* dry density. The detailed results of cement-stabilized macadam are given in Table 3.

2.3.2 7 d Unconfined compressive strength

The mechanical properties of cement-stabilized macadam were evaluated by using the unconfined compressive strength test. The dimensions of specimens were 150 mm in diameter and 150 mm in height. The specimens were tested at 20°C at a loading rate of 1 mm/min after the specimens were cured for 28 d under the standard condition. The unconfined compressive strength values were calculated according to the respective failure loads. Nine replicate specimens were be tested to ensure the reliability and accuracy of every average result.

2.3.3 Flexural strength

All the specimens were prepared by compacting at the respective maximum dry density and optimum moisture content. A series of beam specimens with the size of 100 mm × 100 mm × 400 mm were used to determine the flexural strength. The specimens were tested at 20°C at a loading rate of 0.05 mm/min after the specimens were cured for 28 d under the standard condition. Six replicate specimens were tested to ensure the reliability and accuracy of every average result. The test apparatus of flexural strength is presented in Figure 3.

2.3.4 Dry shrinkage

The specimens for the dry shrinkage test were made into transoms of 100 mm × 100 mm × 400 mm. After the samples were cured at standard conditions for 7 d, they were moved to the environment room at 20°C and 60% RH for the dry shrinkage test. The samples were placed and secured in the retraction equipment as shown in Figure 4, and the data were recorded continuously for 30 d. These data were used to get the water loss rate and dry shrinkage strain based on Eq. 1 and Eq. 2, respectively.

$$\text{Water loss rate: } w_i = (m_i - m_{i+1})/m_p, \quad (1)$$

$$\text{Dry shrinkage strain: } \varepsilon_i = (\overline{X_i} - \overline{X_{i+1}})/L0, \quad (2)$$

where w_i is the water loss rate of the i-th test; m_i is the i-th tested mass of the specimen; m_p is the mass of the dried specimens; ε_i is the dry shrinkage strain of the i-th test; X_i is the length of the i-th measurement; and $L0$ is the length of the specimen.

3 Results and discussion

3.1 Mechanical strength

The mechanical strength of cementitious materials is shown in Figure 5. As shown, the compressive strength of the SWCM increases with the curing days, the early strength is lower than that of ordinary Portland cement (OPC), but the later strength exceeds that of OPC. The compressive strength of the SWCM is much lower than that of OPC, with a compressive strength of 14.3 MPa at 3 d. The compressive strength of the SWCM is higher than that of OPC after 7 d. The compressive strength of the SWCM reaches 52.3 MPa, which is 12.2% higher than that of

TABLE 3 Compaction test results of stabilized macadam.

Cementitious material content (%)	SWCM		OPC	
	Optimum water content (%)	Maximum dry density (g/cm^3)	Optimum water content (%)	Maximum dry density (g/cm^3)
3	3.8	2.307	3.6	2.310
4	4.7	2.315	4.4	2.318
5	5.5	2.324	5.5	2.327
6	6.2	2.333	5.9	2.335

According to the above maximum dry density and optimum water content, the mixtures were filled into the molds and compacted by using a static compression machine to achieve 98% maximum dry density. The compacted samples were demolded after 24 h.

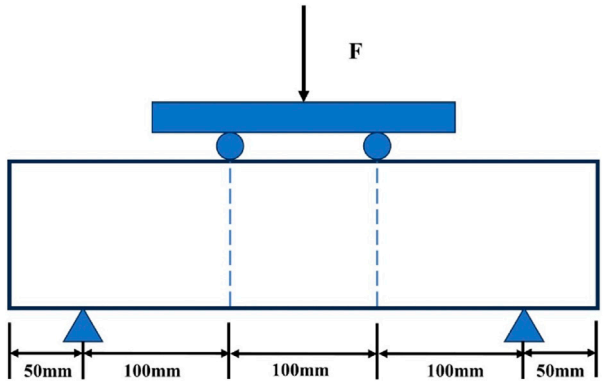

FIGURE 3
Schematic representation of the flexural strength test.

FIGURE 4
Drying shrinkage measuring instrument.

OPC at 28 d. The increased regulation of flexural strength is similar to that of compressive strength, and the flexural strength gradually increases with curing age. The early flexural strength of the SWCM is comparable to that of OPC, and after curing for 7 d, the flexural strength becomes much higher than that of OPC, reaching 6.8 MPa. The flexural strength at 28 d is 9.2 MPa, which is 22.7% higher than that of OPC. Comparing the two cementitious materials, the flexural and compressive strength ratios of the SWCM is higher than that of OPC at all ages, which is attributed to its higher flexural strength.

3.2 Isothermal calorimetric method

The hydration process of the SWCM and OPC can be monitored by using the isothermal calorimetric method, in which the hydration process is reflected by hydration heat flow and total heat. The hydration heat flow and total heat of the SWCM and OPC within 100 h are shown in Figure 6. It can be seen that the hydration rate of the SWCM is slower and less exothermic than that of OPC. The hydration heat flow of the SWCM and OPC is very high during the first minutes, which is mainly attributed to ionic dissolution and the reaction of calcium aluminate with gypsum. After the initial hydration period, the heat flow becomes slower, and the hydration reaction enters the induction period. The induction period of the SWCM is very long, approximately 30 h, which is about five times longer than that of OPC, which is approximately 6 h. The second exothermic peak of the hydration reaction follows the accelerated period, and the second exothermic peak of OPC occurs at 23 h, with a heat flow value of 1.88 mw/g. However, the second exothermic peak of the SWCM is prolonged and is approximately 17 h, and the heat flow value is 1.09 mw/g at 40 h. Then, the heat flow value of the SWCM is higher than that of OPC. The total heat of OPC before 10 h is low, while it increases greatly later. The exothermic heat of the SWCM hydration exceeds 250 J/g within 100 h. Before approximately 35 h, the total heat of the SWCM is low, up to 100 h, and its total heat reaches 150 J/g, which is approximately 60% that of OPC. Lower exothermic hydration can reduce temperature stress and maintain specimen volume stability.

3.3 Microstructure of pastes

Figure 7 represents the XRD patterns of SWCM and OPC pastes at the curing age of 7 d and 28 d, respectively. For OPC, the main crystalline product of hydration is calcium hydroxide (CH), and with the prolongation of the hydration, the diffraction peaks of silicate minerals weaken, while the diffraction peaks of CH continue to increase. It can be seen that the main crystal hydration products of SWCM pastes at 7 d are AFt and unreacted gypsum. The AFt

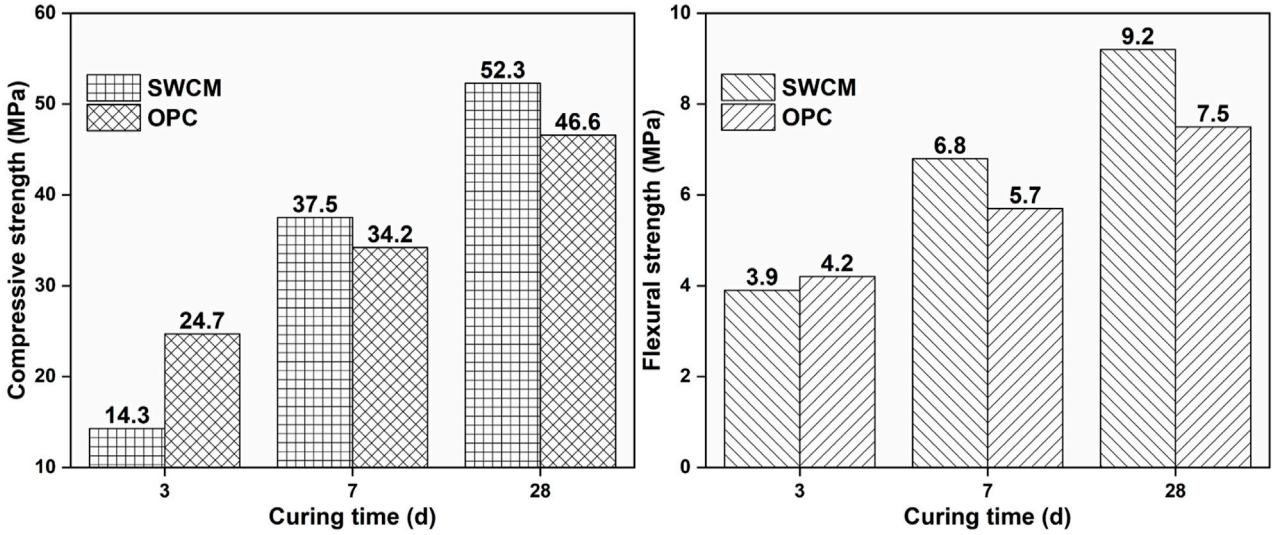

FIGURE 5
Mechanical strength of SWCM and OPC.

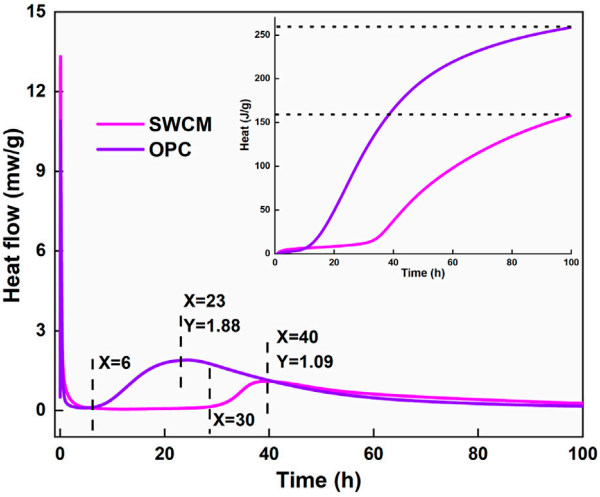

FIGURE 6
Isothermal calorimetric measurements of SWCM and OPC.

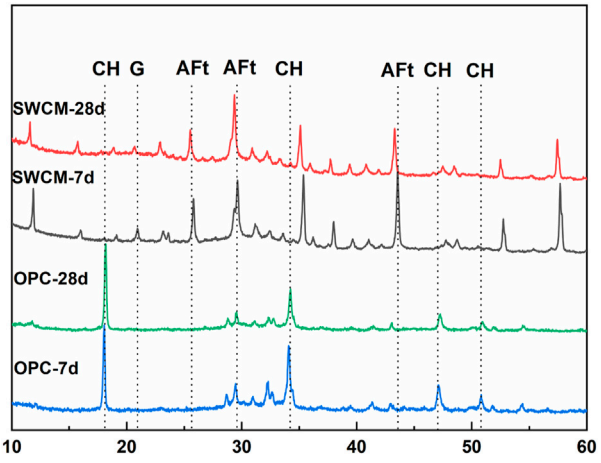

FIGURE 7
XRD patterns of samples in different curing ages.

diffraction peak of the SWCM specimen enhances and the gypsum diffraction peak weakens at the curing age of 28 d, which indicates that a large amount of gypsum is consumed to produce AFt. According to Figure 6, the hydration reactivity of the SWCM is very slow at an early age, which affects the formation of hydration products.

Figure 8 shows the morphology of hydration products of OPC and the SWCM at 7 d and 28 d, respectively. A large amount of hexagonal-like CH and a small amount of needle-like AFt are presented on the surface of the OPC specimens at 7 d, while a large amount of unreacted cement clinker is embedded in the pastes. This is in agreement with the XRD results given in Figure 7. For the SWCM, the needle-like AFt is found to grow up and fill the pores in the pastes under SEM. Besides, a lot of C-S-H gel is also found at 28 d, and the needle-like AFt is wrapped by C-S-H gel, forming a relatively denser structure. A large number of needle-like AFt forms a spatial reticulation structure, reaching the role of fiber reinforcement and improving the flexural strength, which also reveals the reason for the high ratio of flexural and compressive strength of the SWCM.

The SWCM is a cementitious material that utilizes gypsum and CH to activate the potential hydraulic reactivity of slag to produce AFt, which improves flexural strength and achieves micro-expansion (Liu et al., 2019; Liu et al., 2020). The simplified hydration process of the SWCM is demonstrated in Eq. 3 (Angulski da Luz and Hooton, 2019). A proportion of cement clinker occurs initially encountering water, providing CH, which promotes the dissolution of Ca^{2+} and Al^{3+} in the slag. The reactive

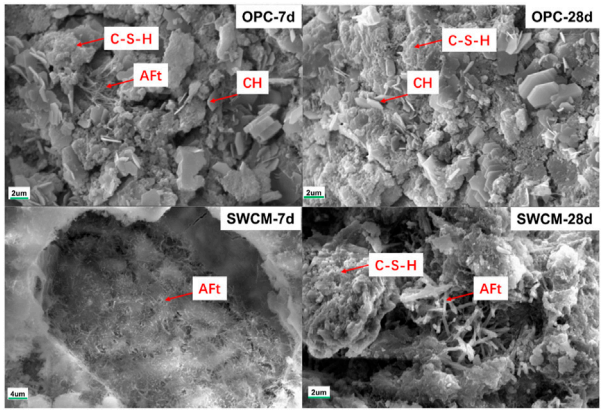

FIGURE 8
Samples in different curing ages under SEM.

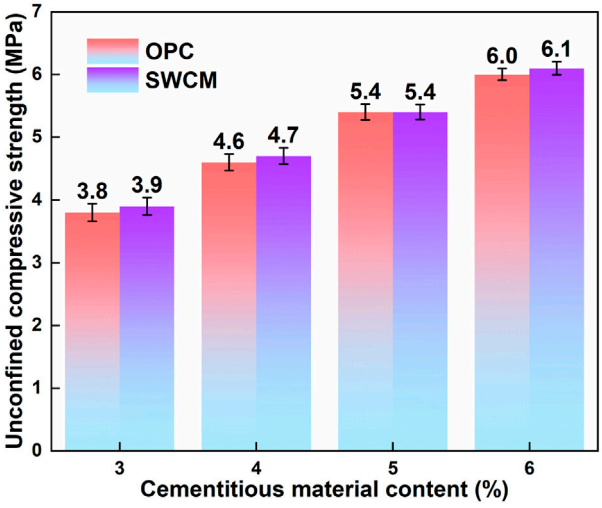

FIGURE 9
Relationship between unconfined compressive strength and cementitious material type and content.

Ca^{2+} and Al^{3+} react with the calcium sulfate from gypsum forming AFt and C-S-H gel.

$$C_5S_3A + CH + C\$ + H \rightarrow C - S - H + AFt. \quad (3)$$

3.4 7 d Unconfined compressive strength

Figure 9 shows the unconfined compressive strength of samples with different cementitious materials. It can be seen from Figure 9 that the 7 d unconfined compressive strength is increased with increasing content of cementitious materials. The strength representative value of the specimen reaches 4.7 MPa when the dosage of the SWCM is 4%, which is comparable to OPC-stabilized macadam. All of the specimens satisfy the strength requirements for roadbases of highways in the Technical Guidelines for Construction

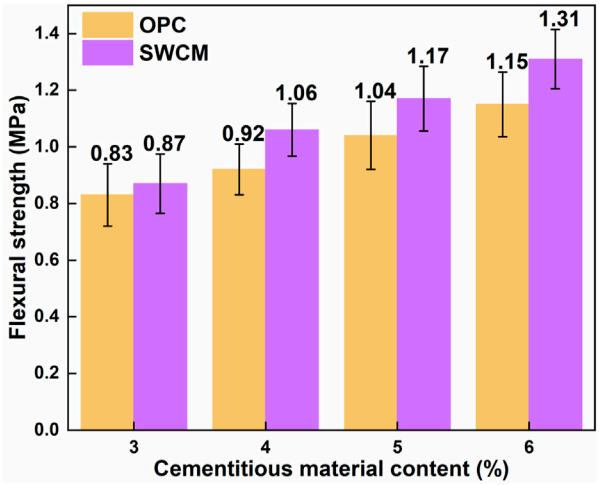

FIGURE 10
Relationship between flexural tensile strength and cementitious material type and content.

of Highway Roadbases (JTG/T F20-2015). The strength value of the stabilizing macadam mainly depends on the following three aspects (Liang et al., 2020): first, the skeleton embedding effect between coarse aggregates; second, the filling effect of fine aggregates; and third, the bonding effect from the cementitious material and the aggregates. Under the same condition of grading, the increase in binder dosage improves the bonding effect between the cementitious material and aggregates, which makes the 7 d unconfined compressive strength value of the specimen increase further. Comparing the two cementitious materials, the representative values of the unconfined compressive strength of SWCM-stabilized aggregates at the same dosage are comparable to that of OPC.

3.5 Flexural strength

Figure 10 \shows that the cementitious material is one of the important factors affecting the flexural strength of stabilizing macadam materials. The flexural strength of the stabilizing macadam increases linearly with increasing content of cementitious materials. The flexural strength of the OPC-stabilized macadam increases from 0.83 MPa to 1.15 MPa when the OPC content increases from 3% to 6%, a 38.5% increase. The flexural strength of the SWCM-stabilized macadam increases from 0.87 MPa to 1.31 MPa when the SWCM content increases from 3% to 6%, a 33.5% increase. Comparing the results of the flexural tensile strength of the two cementitious material-stabilized macadam, the ability of SWCM-stabilized macadam materials to resist bending and tensile deformation is better than that of OPC-stabilized cement, and the bending and tensile strength of the SWCM-stabilized macadam are increased by approximately 15% at the dosage of 4%, which is related to the hydration products of the two cementitious materials. This is corroborated by the SEM and XRD results.

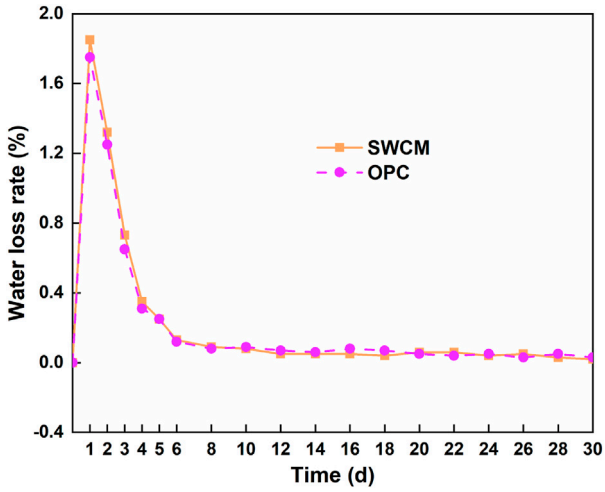

FIGURE 11
Water loss rate of the dry shrinkage test.

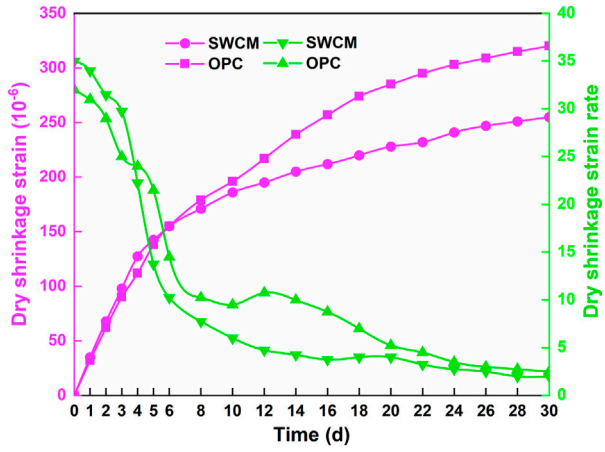

FIGURE 12
Variation of dry shrinkage strain and dry shrinkage strain rate with time.

3.6 Dry shrinkage

The dry shrinkage is an important index to measure the crack resistance and deformation characteristics of stabilized macadam, so it is necessary to analyze the dry shrinkage property of cement-stabilized macadam (Sun et al., 2022b). In this study, we compared the dry shrinkage property of SWCM-stabilized macadam and OPC-stabilized macadam by using 4% of the cementitious material as an example.

Figure 11 shows the results of water loss with age for the two cementitious material-stabilized macadam. Most of the water loss occurs in the first 6 days of the dry shrinkage test and decreases with the extension of the test age. The rate of water loss decreases gradually at the early age and stabilizes at the later age. This is due to the fact that the cement-stabilized macadam specimens contain free water, which evaporates first, followed by capillary water, resulting in a higher rate of water loss at the early test. The water loss rate of SWCM-stabilized macadam is higher than that of OPC-stabilized macadam at the early test, which is caused by its high optimum water content.

Figure 12 shows the variation of dry shrinkage strain and dry shrinkage strain rate with time for the two cementitious material-stabilized macadam. The dry shrinkage strain rate is the first-order derivative of the dry shrinkage strain, and the larger the value, the faster the change of dry shrinkage strain. From the results shown in Figure 12, it can be seen that the dry shrinkage strain increases gradually with an increase in curing age, and the dry shrinkage strain rate decreases gradually. This indicates that the dry shrinkage strain tends to level off, which is more obvious after the 10th day. The SWCM-stabilized macadam is a much smaller dry shrinkage strain than OPC-stabilized macadam. The difference between the two cementitious material-stabilized macadam increases with time. At the end of the test, the dry shrinkage strain of the SWCM-stabilized macadam is 255×10^{-6}, which is only 79.7% of the dry shrinkage strain of the OPC-stabilized macadam, which is 320×10^{-6}. The dry shrinkage strain is related to the hydration products of cementitious materials, and the composition of the hydration products of the SWCM materials is different from that of OPC.

4 Conclusion

In this work, SWCM is prepared by using slag, fly ash, desulfurization gypsum, and gangue. In the process of further discussing the unconfined compressive strength, flexural tensile strength, and dry shrinkage of stabilizing macadam, the following conclusions can be drawn:

(1) The compressive strength of the SWCM increases with the curing days, the early strength is lower than that of OPC, but later the strength exceeds that of OPC.
(2) The hydration rate of the SWCM is slower and less exothermic than that of OPC. The exothermic heat of hydration of the SWCM is approximately 60% that of OPC within 100 h.
(3) Microstructure results show that the hydration products of the SWCM are mainly AFt and C-S-H gel, and a large number of AFt intertwines to form a skeleton, which improves the bending and tensile strength.
(4) The 7 d unconfined compressive strength of the SWCM-stabilized macadam material is comparable to that of the OPC-stabilized macadam, and the 7 d unconfined compressive strength of the 4% SWCM meets the specification of roadbases' strength requirements.
(5) The ability of the SWCM-stabilized macadam to resist bending and tensile deformation is better than that of OPC-stabilized macadam, and the bending and tensile strength are increased by approximately 15% at the dosage of 4%.
(6) SWCM-stabilized macadam is a much smaller dry shrinkage strain than OPC-stabilized macadam. The dry shrinkage strain of SWCM-stabilized macadam is only 79.7% of OPC-stabilized macadam.

Data availability statement

The original contributions presented in the study are included in the article/Supplementary Material; further inquiries can be directed to the corresponding author.

Author contributions

FC: Data curation, investigation, methodology, and manuscript writing–original draft. CL: Conceptualization and manuscript writing–review and editing. CW: Data curation, investigation, methodology, and manuscript writing–original draft. YW: Conceptualization, formal analysis, project administration, and manuscript writing–review and editing.

Funding

The authors declare that financial support was received for the research, authorship, and/or publication of this article. This study was financially supported by the Shandong Province Key R&D Program (Major Technological Innovation) (No. 2020CXGC011405). The authors gratefully acknowledge their financial support.

Conflict of interest

Authors FC and CW were employed by Shandong Hi-speed Construction Management Group Co., Ltd. Author CL was employed by Shandong Hi-Speed Engineering Testing Co., Ltd.

The remaining authors declare that the research was conducted in the absence of any commercial or financial relationships that could be construed as a potential conflict of interest.

Publisher's note

References

Angulski da Luz, C., and Hooton, R. D. (2019). Influence of supersulfated cement composition on hydration process. *J. Mater. Civ. Eng.* 31 (6), 04019090. doi:10.1061/(asce)mt.1943-5533.0002720

Deng, C., Jiang, Y., Yuan, K., Tian, T., and Yi, Y. (2020). Mechanical properties of vertical vibration compacted lime–fly ash-stabilized macadam material. *Constr. Build. Mater.* 251, 119089. doi:10.1016/j.conbuildmat.2020.119089

Dobiszewska, M., Bagcal, O., Beycioğlu, A., Goulias, D., Köksal, F., Płomiński, B., et al. (2023). Utilization of rock dust as cement replacement in cement composites: an alternative approach to sustainable mortar and concrete productions. *J. Build. Eng.* 69, 106180. doi:10.1016/j.jobe.2023.106180

Grabias-Blicharz, E., and Franus, W. (2023). A critical review on mechanochemical processing of fly ash and fly ash-derived materials. *Sci. Total Environ.* 860, 160529. doi:10.1016/j.scitotenv.2022.160529

Griffiths, S., Sovacool, B. K., Del Rio, D. D. F., Foley, A. M., Bazilian, M. D., Kim, J., et al. (2023). Decarbonizing the cement and concrete industry: a systematic review of socio-technical systems, technological innovations, and policy options. *Renew. Sustain. Energy Rev.* 180, 113291. doi:10.1016/j.rser.2023.113291

Guo, Y., Luo, L., Liu, T., Hao, L., Li, Y., Liu, P., et al. (2023). A review of low-carbon technologies and projects for the global cement industry. *J. Environ. Sci.* 136, 682–697. doi:10.1016/j.jes.2023.01.021

Ju, C., Liu, Y., Yu, Z., and Yang, Y. (2019). Cement-lime-fly ash bound macadam pavement base material with enhanced early-age strength and suppressed drying shrinkage via incorporation of slag and gypsum. *Adv. Civ. Eng.* 2019, 1–10. doi:10.1155/2019/8198021

Koralegedara, N. H., Pinto, P. X., Dionysiou, D. D., and Al-Abed, S. R. (2019). Recent advances in flue gas desulfurization gypsum processes and applications–A review. *J. Environ. Manag.* 251, 109572. doi:10.1016/j.jenvman.2019.109572

Li, W., Lang, L., Lin, Z., Wang, Z., and Zhang, F. (2017). Characteristics of dry shrinkage and temperature shrinkage of cement-stabilized steel slag. *Constr. Build. Mater.* 134, 540–548. doi:10.1016/j.conbuildmat.2016.12.214

Liang, C., Wang, Y., Tan, G., Zhang, L., Zhang, Y., and Yu, Z. (2020). Analysis of internal structure of cement-stabilized macadam based on industrial CT scanning. *Adv. Mater. Sci. Eng.* 2020, 1–10. doi:10.1155/2020/5265243

Liu, S., Fang, P., Ren, J., and Li, S. (2020). Application of lime neutralised phosphogypsum in supersulfated cement. *J. Clean. Prod.* 272, 122660. doi:10.1016/j.jclepro.2020.122660

Liu, S., Wang, L., and Yu, B. (2019). Effect of modified phosphogypsum on the hydration properties of the phosphogypsum-based supersulfated cement. *Constr. Build. Mater.* 214, 9–16. doi:10.1016/j.conbuildmat.2019.04.052

Matthes, W., Vollpracht, A., Villagrán, Y., Kamali-Bernard, S., Hooton, D., and Gruyaert, E. (2018). Ground granulated blast-furnace slag. Properties of fresh and hardened concrete containing supplementary cementitious materials: state-of-the-art report of the RILEM technical committee 238-SCM. *Work. Group* 4, 1–53. doi:10.1007/978-3-319-70606-1_1

Mo, L., Zhang, F., Panesar, D. K., and Deng, M. (2017). Development of low-carbon cementitious materials via carbonating Portland cement–fly ash–magnesia blends under various curing scenarios: a comparative study. *J. Clean. Prod.* 163, 252–261. doi:10.1016/j.jclepro.2016.01.066

Ou-Ming, X. U., Shi-Heng, W., Min, B., Xuan, L., and Lian-Cheng, Z. (2019). Influence of fly ash and granulated blast furnace slag on strength and shrinkage characteristics of cement stabilized crushed stone. *J. Guangxi Univ. Nat Sci Ed)* 44 (2), 509–515. doi:10.13624/j.cnki.issn.1001-7445.2019.0509

Qian, G., Zhong, Y., Li, X., Peng, H., Su, J., and Huang, Z. (2022). Experimental study on the road performance of high content of phosphogypsum in the lime–fly ash mixture. *Front. Mater.* 9, 935113. doi:10.3389/fmats.2022.935113

Qing-qing, L. U. (2021). Strength enhancement and shrinkage reduction mechanism of desulfurized gypsum cement stabilized aggregates. *J. Jilin Univ. Technol. Ed.* 51 (1), 252–258. doi:10.13229/j.cnki.jdxbgxb20200242

Sun, C., Zhang, J., Yan, C., Yin, L., Wang, X., and Liu, S. (2022a). Hydration characteristics of low carbon cementitious materials with multiple solid wastes. *Constr. Build. Mater.* 322, 126366. doi:10.1016/j.conbuildmat.2022.126366

Sun, Y., Li, L., Liao, J., and Huang, C. (2022b). Dry shrinkage performance of cement-stabilized reclaimed lime-fly ash macadam. *Constr. Build. Mater.* 331, 127332. doi:10.1016/j.conbuildmat.2022.127332

Wang, Y., Xu, L., He, X., Su, Y., Miao, W., Strnadel, B., et al. (2022). Hydration and rheology of activated ultra-fine ground granulated blast furnace slag with carbide slag and anhydrous phosphogypsum. *Cem. Concr. Compos.* 133, 104727. doi:10.1016/j.cemconcomp.2022.104727

Wiranata, D. Y., Yang, S. H., Akgul, C. M., Hsien, H. Y., and Nugraha, M. Z. P. (2022). Use of coal ash cement stabilized material as pavement base material: laboratory characterization and field evaluation. *Constr. Build. Mater.* 344, 128055. doi:10.1016/j.conbuildmat.2022.128055

Xu, L., Wang, J., Li, K., Li, M., Lin, S., Hao, T., et al. (2023). Investigations on the rehydration of recycled blended SCMs cement. *Cem. Concr. Res.* 163, 107036. doi:10.1016/j.cemconres.2022.107036

Zhang, J., Tan, H., Bao, M., Liu, X., Luo, Z., and Wang, P. (2021). Low carbon cementitious materials: sodium sulfate activated ultra-fine slag/fly ash blends at ambient temperature. *J. Clean. Prod.* 280, 124363. doi:10.1016/j.jclepro.2020.124363

Zhao, H. X., Zhou, F. S., Lm, A. E., Liu, J. L., and Zhou, Y. (2022). A review on the industrial solid waste application in pelletizing additives: composition, mechanism and process characteristics. *J. Hazard. Mater.* 423, 127056. doi:10.1016/j.jhazmat.2021.127056

Zhao, J., Wang, D., Yan, P., Zhang, D., and Wang, H. (2016). Self-cementitious property of steel slag powder blended with gypsum. *Constr. Build. Mater.* 113, 835–842. doi:10.1016/j.conbuildmat.2016.03.102